Dipole strength function in ^{11}Li

G. Bertsch and J. Foxwell
Department of Physics and Cyclotron Laboratory, Michigan State University, East Lansing, Michigan 48823
(Received 6 October 1989)

The dipole response of the neutron-rich nucleus ^{11}Li is calculated in the random phase approximation and compared with the recent experimental measurement of Coulomb breakup by Kobayashi *et al.* While the theory predicts a softening of the dipole mode as expected, the response is not sufficiently enhanced to explain the experimental data. This shows the need for a theory that deals with correlations beyond those included in random phase approximation.

Recent experiments by Tanihata *et al.*[1] showed that the nucleus[11] Li has a large fragmentation cross section on high-Z targets, which may be attributed to Coulomb excitation and breakup. The extracted Coulomb excitation cross section for the reaction ^{208}Pb(^{11}Li,^{9}Li) with an 800 MeV/nucleon beam is 0.9 ± 0.1 b. Such a large cross section requires that the dipole response of the nucleus be greatly enhanced at low excitation. Qualitatively such an effect is expected because nearly unbound neutrons extend beyond the usual nuclear radius. These neutrons do not couple strongly to the motion of the core, and thus lose less of their strength to the giant dipole resonance.[2] The entire strength function, including the giant dipole as well as the low contribution of the weakly bound nucleons, may be calculated in the random phase approximation (RPA). While the validity of the RPA may be questioned because it only includes a small class of correlations, it is nevertheless a useful limit to understand and compare with other treatments. This work presents an RPA study of the strength function. The coupling of weakly bound neutrons to the dipole mode has also been studied in a hydrodynamic model.[3] In an opposite limit, one may assume that the nucleons are completely correlated into a pair of clusters, and model the wave function as a two-particle system.[4,5]

Our calculations use the program RPA3, which is described in detail in Ref. 6. The algorithm treats the single-particle continuum exactly, and the computed response function satisfies the energy-weighted sum rule. In the program, a set of single-particle wave functions is constructed using a Woods-Saxon potential. We use the Woods-Saxon functions in the calculations described here, but we have also constructed Hartree-Fock states with nearly identical results. The program was modified slightly to allow adjustment of the Woods-Saxon potential, and also to treat open shell nuclei via the spherical RPA with partial occupation of the shells.

The nucleus ^{11}Li has a filled neutron major shell, with the neutron removal energy of only 0.19 MeV. We ascribe these weakly bound neutrons to the $p_{1/2}$ shell, and choose the parameters of the Woods-Saxon potential accordingly. Thus, the energy of the $p_{1/2}$ neutron orbit is taken to be -0.19 MeV. This prescription overestimates the extent to which the neutron density spreads out: ^{10}Li with one neutron in the $p_{1/2}$ shell is unbound by about 1 MeV, so the separation energy to leave the remaining neutron in the $p_{1/2}$ is about 1 MeV. Since our basic approximation cannot distinguish between these, we shall consider Woods-Saxon potentials for both separation energies. We expect that a more fundamental treatment with correlation effects would produce wave functions with some intermediate falling off. The parameters of the Woods-Saxon potential are quoted in Table I.

The existence of a spurious state in the RPA, associated with the translational degeneracy of the ground state, causes a technical problem in our calculation. In principle, the spurious state should not couple to the intrinsic dipole operator, which is given by

$$M(E1,m)=\frac{N}{A}\sum_{p} r_p Y_{1,m}-\frac{Z}{A}\sum_{n} r_n Y_{1,m} \ . \tag{1}$$

This may be easily seen by integrating $M(E1)$ over the transition density of the spurious state, $\delta\rho^{p,n}(r)=\nabla\rho_0^{p,n}$. However, due to lack of self-consistency between the residual interaction and the static potential field, this relation is not exactly fulfilled numerically and the dipole operator appears to couple to the spurious state. This problem is easily remedied by adjusting the isoscalar interaction to move the spurious state away from the threshold region of the response.

We next briefly discuss the residual interaction. In the isoscalar channel, the interaction is strongly constrained by self-consistency, but it has essentially no effect on the response apart from the spurious coupling mentioned above. In the isovector channel, the interaction is a density-dependent contact interaction. For simplicity we use a density-independent form,

$$v=\sum_{i<j}\tau_i\cdot\tau_j v_\tau\delta(r_i-r_j) \tag{2}$$

with $v_\tau=350$ MeV fm^3. The interaction strength is chosen as a compromise between a value that fits the symmetry energy of nuclear matter and a value that fits the giant dipole in ^{16}O. This interaction strength yields a giant dipole at approximately the correct energy in heavy nuclei.

The computed dipole response for the above Hamiltonian parameters, having the occupied $p_{1/2}$ neutron orbital bound by 0.2 MeV, is graphed in Fig. 1. The solid

TABLE I. Parameters of the Woods-Saxon well.

$U_{n,p}(r)=V_{n,p}f(r)+l\sigma V_{ls}f'(r)/r$; $f(r)=1/\{1+\exp[(r-R)/a]\}$.
$V_n=-35.95$ MeV
$V_p=-57.76$ MeV
$V_{ls}=-15.5$ MeV fm
$a=0.65$ fm
$R=2.78$ fm

line shows the single-particle response without interactions. The main features are a broad peak around 15 MeV associated with $1\hbar\omega$ transitions, and a low continuum starting at the neutron threshold. The RPA response, shown as the dashed line, has the strength shifted upward, with about half of the energy-weighted sum in a peak at 22 MeV. There is much less collectivity here than for $N=Z$ nuclei. At low excitation, the continuum is suppressed by about 20% with respect to the single-particle model. This suppression is quite mild compared to normal low $E1$ transitions.[7] As mentioned earlier, the coupling to the giant dipole is rather weak because transition density is peaked in the far surface.

To calculate the Coulomb excitation cross section, we use the formula for the dipole excitation probability by a relativistic Coulomb field, which is derived in Ref. 8 or 9. The probability P to excite the nucleus depends on the impact parameter b, the transition energy E, the charge of the Coulomb field Z, and the velocity of the projectile v and its Lorentz dilation factor γ as follows:

$$P(b)=\frac{16\pi Z^2e^4B(E1,\uparrow)\xi^2}{9\hbar^2v^2b^2}[K_1^2(\xi)+K_0^2/\gamma^2] . \quad (3)$$

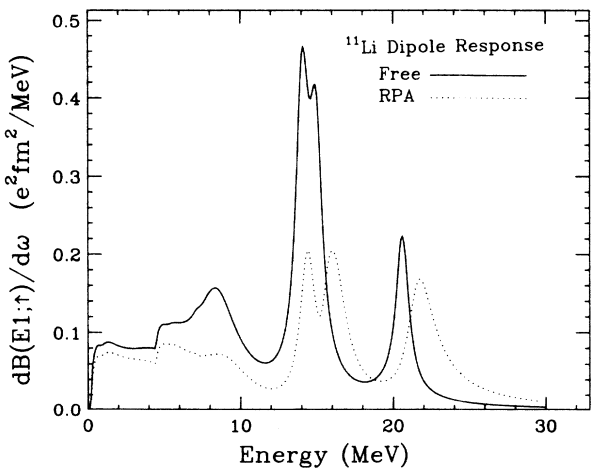

FIG. 1. The electric dipole strength distribution in ^{11}Li predicted in the RPA. The solid line shows the free response and the dashed line the RPA response. To make the bound-to-bound state transitions in the free response visible on the graph, the response was smoothed above 7 MeV excitation, giving the states an artificial width of 1 MeV.

Also $\xi=Eb/\hbar\gamma v$ is the adiabaticity parameter, and the dipole transition strength $B(E1;\uparrow)$ is the square of the matrix element (1) summed over m states of the operator and the final state. The cross section is given by

$$\sigma=\int_{b_0}^{\infty}P(b)2\pi b\,db . \quad (4)$$

Evaluating this for the conditions of the experiment in Ref. 1, i.e., a beam energy of 800 MeV/nucleon and $Z=82$ Coulomb field and $b_0=11$ fm, we find that the cross section is given to within 10% by the formula

$$\sigma\simeq 9.1B(E1;\uparrow)\ln[(18.8\text{ MeV}/E)^2+1] . \quad (5)$$

In Eq. 5, the $B(E1)$ and the cross section have the same units, i.e., fm^2 or mb. We integrate the cross section per unit $B(E1)$ from Eq. (5) over the RPA strength function to obtain the predicted Coulomb excitation cross section.

The RPA prediction for valence neutrons bound by 0.19 MeV is 0.28 b, too small by a factor of 3. The disagreement is even worse if the neutron separation energy is set at 1.0 MeV. This leads us to question the assumption that the neutrons are in the $p_{1/2}$ orbit. Certainly there are important correlation effects that will require the single-particle wave functions to be distributed over many angular momenta. If the particles are in the $s_{1/2}$ orbit, the wave function can extend much farther from the nucleus because there is no centrifugal barrier. Also, we note that in the nucleus ^{11}Be, the spin values of the ground and first excited states ($\frac{1}{2}+$ and $\frac{1}{2}-$, respectively) suggest that the $s_{1/2}$ orbit may be below the $p_{1/2}$. We thus examine the consequences of an inversion of these two states. It is not easy to make the $s_{1/2}$ more bound than the $p_{1/2}$ within a Woods-Saxon model, but we were able to do this by increasing the strength of the spin-orbit interaction by a factor of 4, and changing the diffusivity of the well from 0.65 to 1.0 fm. Adjusting the central interaction to make the $s_{1/2}$ bound by 0.19 MeV, and the $p_{1/2}$ unbound by 1 MeV, we find an enhanced cross section, listed in Table II along with the other values. The s-wave valence neutron gives a cross section much larger than the other estimates, but it is still smaller than the experimental breakup cross section.

We have thus shown that the Coulomb breakup of ^{11}Li would be very difficult to explain in the framework of the conventional shell model. In a cluster model, such as considered in Refs. 4 and 5, the possibilities are greater. The energy-weighted sum rule for clusters[10] allows 8% of

TABLE II. Coulomb excitation cross section for 800 MeV/nucleon ^{11}Li on ^{208}Pb target in various models, compared to experiment.

Valence neutron orbit	Binding energy (MeV)	Cross section (b)
$p_{1/2}$	0.19 MeV	0.28
$p_{1/2}$	1.0 MeV	0.19
Experimental		$>0.9\pm0.1$

the normal sum in ^{11}Li to be in the ^{9}Li$+2n$ channel. This amounts to 2.7 MeV fm^2, which could explain the data if the strength were concentrated below a few MeV's. More realistic calculations are needed, which may well require techniques from three-body theory.

This work was supported by the National Science Foundation under Grant No. PHY 87-14432.

[1]T. Kobayashi *et al.*, Phys. Lett. B **232**, 51 (1989).
[2]T. Uchiyama and H. Morinaga, Z. Phys. A **320**, 273 (1985).
[3]Y. Suzuki, K. Ikeda, and H. Sato, University of Michigan report, 1989.
[4]P. Hansen and B. Johnson, Europhys. Lett. **4**, 409 (1987).
[5]C. Bertulani and G. Baur, Nucl. Phys. **A480**, 615 (1988).
[6]G. Bertsch, in *Computational Nuclear Physics* (Springer, Berlin, to be published). Copies of the program with documentation are available from the author. The algorithm is based on S. Shlomo and G. Bertsch, Nucl. Phys. **A243**, 507 (1975).
[7]A. Bohr and B. Mottelson, *Nuclear Structure* (Benjamin, New York, 1975), Vol. 2, p. 488.
[8]J. D. Jackson, *Classical Electrodynamics* (Wiley, New York, 1962), Eq. 13.31.
[9]A. Winther and K. Alder, Nucl. Phys. **A319**, 518 (1979); Eq. 2.15 and Appendix B.
[10]Y. Alhassid *et al.*, Phys. Rev. Lett. **49**, 1482 (1982).